SSC19-IV-08

System Design of the Miniaturized Distributed Occulter/Telescope (mDOT) Science Mission

Simone D'Amico, Adam Koenig, Bruce Macintosh
Stanford University
450 Serra Mall, Stanford, CA 94305
+1 650 497 4682
damicos@stanford.edu

David Mauro
KBR/NASA Ames Research Center
M/S 202-3, Moffett Field, CA 94035
+1 650 604 4775
david.mauro@nasa.gov

ABSTRACT

The miniaturized Distributed Occulter Telescope (mDOT) will provide unprecedented detection and direct measurements of brightness of extrasolar dust disks at short visible to ultraviolet wavelengths. The baseline mission will observe over 15 targets using a starshade for high-contrast imaging, blocking the target star with a specially shaped free-flying occulter to allow nearby objects to be detected. mDOT operates on a much smaller scale than flagship NASA missions, with an autonomous formation of two small satellites in sun-synchronous low Earth orbit. An occulter-smallsat (246kg, 192W) carries a precisely manufactured 3m-diameter starshade and a telescope-cubesat (6U, 12kg, 40W) carries a 10cm-diameter telescope. The satellites are launched combined as a secondary payload for a total mission lifetime of 1.1 years. After launch, the occulter-smallsat ejects the telescope-cubesat and maneuvers to establish the desired relative orbit, leaving the spacecraft at slightly different longitudes of ascending node. Relative eccentricity and inclination vector separation provides the baseline for scientific observations at the equator (500 km) and a minimum safe distance perpendicular to the flight direction at all times (>1km). The starshade suppresses the light of the target star by 10^{-7} or more. During a science pass, high-ISP green propellant thrusters on the occulter-smallsat maintain the formation, while differential GNSS is used for cm-accurate relative navigation. Earth's oblateness perturbations are used to precess the orbits and acquire the science targets over the mission lifetime at minimal propellant cost. The mission addresses key NASA science objectives and provide the unique opportunity to mature starshade techniques for future exoplanet missions.

INTRODUCTION

This paper presents the results of a system point design for the miniaturized distributed occulter/telescope (mDOT) science mission conducted by Stanford University and NASA Ames Research Center under contract from the NASA Mission Directorate. mDOT consists of an occulter-smallsat (246kg, 192W) and a telescope-cubesat (6U, 12kg, 40W) launched together as a secondary payload into a sun-synchronous low Earth orbit (98° inclination, local time of the ascending node of noon/midnight, 600km mean altitude). During nominal operations, the telescope images the vicinity of a target star with unprecedented sensitivity in the near-ultraviolet spectrum from within the deep shadow produced by the starshade.

This will allow unprecedented direct measurements of the brightness of extrasolar dust disks at short visible to ultraviolet wavelengths. Dust from asteroids and comets is a crucial component of other solar systems, tracing the presence of planets while also potentially hiding earthlike planets from mid-sized future space imaging missions. mDOT has three primary science objectives. First, it will be capable of providing B-band photometry of known young massive debris disks detected at longer wavelengths, providing color information to constrain particle sizes. Second, it will attempt to resolve scattered light from disks so far only detected through thermal emission. Finally, it will search for zodiacal dust analogs around nearby stars at a sensitivity level of 5-10 times the solar dust density. mDOT will also serve as a technology demonstrator of starshade techniques for future probe and flagship exoplanet missions and for autonomous formation-flying of small satellites as

enabler of entirely new classes of low-cost, high-impact distributed space telescopes.

This paper presents a rigorous point design for the mission which closes with healthy margins on all relevant technical budgets, increasing the concept maturity level of mDOT. Specifically, science target selection, optical and orbit design, mission operations, and ground and space segments are addressed all the way to bus and payload subsystem sizing, selection, accommodation, and analysis. Emphasis is also given to the guidance, navigation, and control (GN&C) subsystem and to the unique autonomous aspects of mDOT.

The nominal science plan includes 15 relevant target stars which are directly imaged up to 10 times each for a cumulative exposure time of maximum 50 minutes per target over a period of 1.1 years. The optical system consists of a 3m-diameter starshade at a distance of 500 km from a 10cm-aperture telescope during observations. The starshade is designed to provide a contrast of 10^{-7} or better in the B-band (360-520 nm) within a shadow 30cm in diameter and 10km in length. The telescope uses a tip-tilt mirror to achieve 0.2 arcsecond image stabilization for diffraction-limited imagery. The formation is equipped with a precise relative navigation system that uses differential carrier-phase Global Navigation Satellite System (GNSS) measurements to achieve centimeter-level relative navigation in real-time. The occulter-smallsat is precisely and autonomously controlled to keep the telescope-cubesat within the deepest part of the shadow using a set of eleven 5N green-propellant thrusters with a total delta-v capacity of 940 m/s. The relative orbit is selected to minimize the delta-v cost of observations by ensuring that the formation is aligned in the cross-track direction. Besides the baseline design, this paper identifies key open trades and demonstrates how mDOT can enable valuable science at low cost while providing a compelling demonstration of the capabilities of small spacecraft. Figure 1 provides a graphical illustration of mDOT.

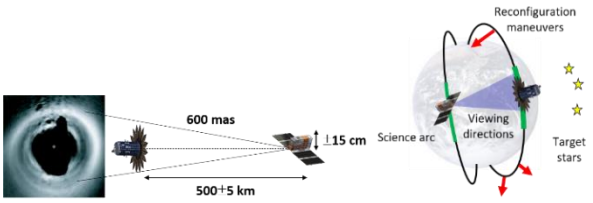

Figure 1: mDOT concept.

REQUIREMENTS

The mDOT mission consists of an autonomous formation in sun-synchronous low Earth orbit (600 km altitude, 98°, noon/midnight local time of the ascending node). The spacecraft are launched together as a single secondary payload compatible with the ESPA Grande ring for a total mission lifetime of 1.1 years. The telescope-cubesat is later deployed from the occulter-smallsat as discussed in the following sections. It is noted that the mission concept is compatible with local times of the ascending node (LTAN) other than noon/midnight as long as one of the nodes of the spacecraft orbits is in eclipse. This corresponds to LTAN in the range of 9AM/9PM-3PM/3AM. A subset of the Mission Traceability Matrix (MTM) is provided in Table 1. As a basic systems engineering tool, the MTM provides a logical flow from mission functional objectives through mission design requirements, spacecraft and platform requirements to operational requirements. The driving requirement for mDOT is the ability for the occulter-smallsat to maintain its relative position with respect to the telescope-cubesat to within ± 10cm perpendicular to the line-of-sight during observations. Thanks to this alignment, the telescope will stay in the deep shadow casted by the starshade and provide direct measurements of brightness of extrasolar dust disks in the near-ultraviolet spectrum.

Table 1: Subset of mDOT MTM.

Mission Functional Requirements	Mission Design Requirements
Optical contrast of 10^{-7}	A starshade shall cast a starlight shadow on an observer telescope orbiting in controlled formation and aligned with the target star.
Inner working angle <1arsec	Baseline separation between spacecraft shall be 500km in cross-track direction with science spectrum of interest of 360-520 nm.
Signal-to-noise-ratio >10	The telescope shall be able to image dust disks with a surface brightness of 21 mag/arcsec^2.
Cumulative exposure 5-50min	The formation relative motion shall be controlled during target star observation to within ±10 cm lateral (perpendicular to line-of-sight) and to within ±5 km longitudinal (along line-of-sight).
Stability of image 0.2arcsec	Telescope camera shall avoid point spread function smearing due to pointing errors and jitter.
Targets within ±10° of nominal declination	The absolute and relative orbits must be selected to ensure that the propulsion system(s) can support the observation of at least 15 science targets. The formation shall align with different targets through passive or active means.

PAYLOADS

The mDOT mission includes two payloads: a telescope hosted on the cubesat and a starshade hosted on the smallsat.

Telescope

The telescope instrument has been designed to meet a resolution of 1.1arcsec or better at 400nm wavelength, with field of view (FoV) larger than 1°. To reduce costs, a search was conducted for off-the-shelf space telescopes with flight heritage that can be repurposed for the mDOT mission and can fit in a 4U volume including the cameras and guiding. Planet Labs offered to make available the design of their telescope for the mDOT mission[1]. The telescope has an aperture of 9.2cm resulting in a resolution of 1.09arcsec, and FoV >1°. Figure 2 shows a simplified schematic version of the telescope. Table 2 lists the key system parameters.

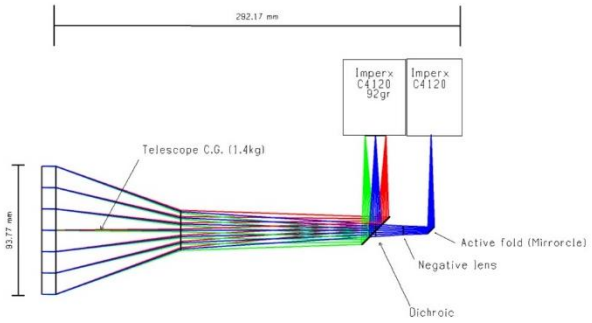

Figure 2: mDOT telescope instrument diagram.

The telescope uses two identical Imperx Cheetah C4120 cameras with 3.45um pixels. The first one, or guiding camera, will sample the FoV and serve as a high-precision star tracker. The second camera will observe the target and will have a negative lens to reach Nyquist sampling. The light will be separated using a dichroic. In this way the guider camera observes wavelengths above 520nm and the science camera observes wavelengths below 520nm. Both cameras will observe the entire FoV but with different plate scale, band, and exposure times. The camera can read out the entire sensor in 12bit at 14Hz, and it has a global shutter with internal and external control that allows reading out without smearing the image. As a result, no mechanical shutter is needed. A tip/tilt Mirrorcle S6180 mirror and piezo actuated mount for the dichroic are used to stabilize the image in the focal plane and avoid smearing due to attitude pointing error. The guiding camera will image background stars with an average of 2.1 stars of apparent magnitude 8 and 8.1 stars with apparent magnitude 9. The pointing information from the background stars will be used to drive the Mirrorcle mirror (active fold) in front of the science camera to stabilize down to 0.2arcsec[2].

Table 2: mDOT telescope key parameters.

Telescope	Parameter	Unit
Aperture	9.2	[cm]
Effective f/#	9	[-]
Focal length	70	[cm]
Weight	1400	[gr]
HFoV	1.484	[deg]
Camera	**Parameter**	**Unit**
Px size	3.45	[um]
Px count	4112	[px]
Mass	91.8	[gr]
FoV	1.2	[deg]
Mass	**Parameter**	**Unit**
Telescope	1400	[g]
Cameras	184	[g]
Optics	70	[g]
Mounts	140	[g]
Harnesses	179	[g]
Total mass	**1973**	**[g]**

In addition, the cubesat attitude determination and control system can receive pointing information from the payload in order to improve the native spacecraft pointing, reducing the stroke and speed of corrections in the active fold. In regular operation each camera consumes 2.6W. A heat pipe connected to the cubesat radiator is necessary to maintain the camera and its detector at ambient temperature.

Starshade

The starshade payload is designed to meet an optical contrast of 10^{-7} or better between 360 and 520 nm and an inner working angle of 0.6arcsec. The starshade design is also subject to constraints to ensure that it is realizable and compatible with the ESPA Grande ring and the mission operation concept (see dedicated sections). Using conventional starshade scaling relations with a desired Fresnel number of 10 in the bandwidth of interest, the designed starshade is 3m in diameter and requires a separation of 500±5km from the telescope to achieve the required contrast[3]. The starshade includes a 1m-diameter central deck mounted to the spacecraft bus and 16 petals each 1m in length. The petal shapes are computed by solving a variant of Vanderbei's optimization problem that maximizes the depth of the shadow produced by the starshade in a specified volume and bandpass[4,5]. There is a gap of 0.5mm between adjacent petals and the petal tips are 1mm-wide to ensure that the design can be manufactured using conventional

techniques. Key parameters of the starshade are listed in Table 3.

Table 3: mDOT starshade key parameters.

Starshade	Parameter	Unit
Diameter	3	[m]
Deck diameter	1	[m]
Petal length	1	[m]
Petal gap width	0.5	[mm]
Petal tip width	1	[mm]
Total mass	23.2	[kg]

Because the combined starshade and telescope must produce an optical contrast of 10^{-7} or better, it is necessary to ensure that the starshade is accurately manufactured and deployed. Collaborators at JPL developed a manufacturing and deployment error budget using the same model used for Exo-S and other full-scale starshades[6]. Detailed specifications are omitted here for brevity. Due to the relaxed contrast requirement as compared to full-scale starshades for exoplanet imaging (which require contrast of 10^{-10} or better), the mDOT starshade has more relaxed manufacturing and deployment tolerances. Specifically, the critical error mode (oscillations in the petal shape) has a tolerance of 0.1mm, which is an order of magnitude larger than the tolerance for full-scale starshades (which call for a 10micron tolerance)[7]. Due to its small size, the mDOT starshade can be constructed with fewer components, making it easier to satisfy these tolerances. The nominal shape of the mDOT's starshade is depicted in Figure 3. To satisfy the volume constraints of the ESPA Grande ring, each petal is attached to a hinge that is folded along the body of the spacecraft bus at launch. More details on the ESPA Grande envelope and design elements that ensure compatibility are described in dedicated sections.

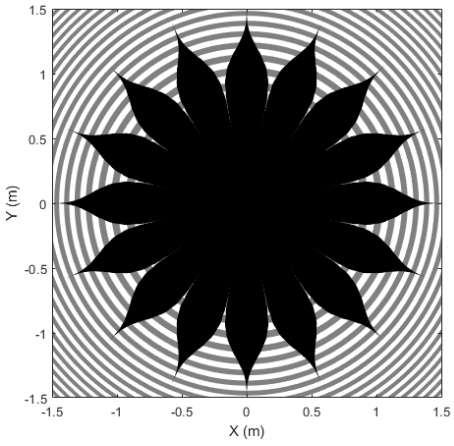

Figure 3: mDOT starshade shape including Fresnel half-zones (gray and white).

MISSION CONCEPT

Mission operations for mDOT are divided into six phases: 1) launch; 2) occulter-smallsat deployment and commissioning; 3) telescope-cubesat deployment and commissioning; 4) formation acquisition; 5) science; and 6) decommissioning. Table 4 lists the major events that the mDOT spacecraft would experience during each of these phases of the mission life cycle. The state of the formation during each of these phases is illustrated in Figure 4. Advancing to the next mission phase requires that all activities associated with the previous mission phase have been performed and satisfied. Phase duration is an estimation based on the number and complexity of events that need to be executed during the phase. A detailed description of each phase is provided in the following sub-sections.

Table 4: mDOT major events.

Phases	Duration	Events
1	<1day	-Stowed occulter-smallsat is carried into sun-synchronous orbit attached to ESPA Grande. -Primary payload is released.
2	2weeks	-ESPA Grande releases occulter-smallsat into sun-synchronous orbit. -Occulter-smallsat conducts validation and calibration process for subsystems, including sensors, actuators, and propulsion system. -Occulter-smallsat conducts data exchange and communications and with mission control center.
3	1week	-Occulter-smallsat ejects telescope-cubesat in cross-track direction per ground command. -Telescope-cubesat conducts validation and calibration process for subsystems, including sensors, actuators, and payloads. -Telescope-cubesat conducts data exchange and communications with occulter-smallsat and control center.
4	4weeks	- Occulter-smallsat maneuvers to achieve 500km cross-track separation from telescope-cubesat through a difference in right ascension of the ascending node. -Occulter- and telescope-spacecraft perform relative navigation to test its performance in preparation for target star observations.
5	11moths	-At least 15 target stars are identified, their observations scheduled, number of revisits established, observation durations estimated. -Occulter-smallsat conducts reconfiguration maneuvers to align with the next target star and formation keeping maneuvers to maintain alignment during observations. -Telescope-cubesat captures image data of the target stars while shadowed by the starshade.

		-Image, health, and orbit data are downloaded, telecommands to both spacecraft are uploaded. -During extended periods of no observation, the telescope-cubesat conducts target pointing to test and calibrate camera sensitivity and image quality.
6	1week	-Occulter-smallsat is commanded to fire its thrusters to reduce its velocity for gradual reentry. -Telescope-cubesat is commanded to orient its solar arrays in the velocity direction to increase drag for gradual reentry. -Science data processing, archival, and publication.

Launch

At launch, the 6U telescope-cubesat will be stowed inside the 6U ISIS DuoPack CubeSat Deployer onboard the occulter-smallsat, integrating the mDOT secondary payload. The mDOT payload attaches to an ESPA Grande launch adapter for ridesharing with a primary payload for launch to a sun-synchronous orbit. Both spacecraft are stowed with inhibited battery power and radio transmissions.

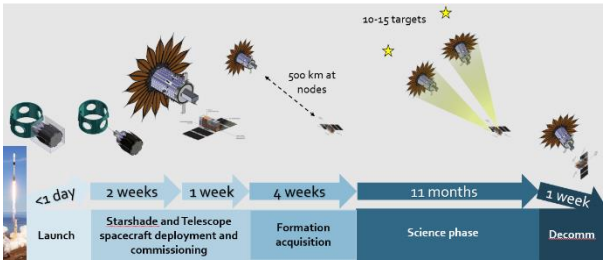

Figure 4: mDOT mission operations phases.

Occulter-smallsat deployment and commissioning

Once ejected from the ESPA Grande, the occulter-smallsat power subsystem is activated by the release mechanism, which in turn provides stand-by power to the other subsystems. The smallsat remains in stowed configuration and may experience tumbling while it develops some distance from the stage. Note that the spacecraft is fully charged prior to integration, and the partial battery charge is sufficient for this short segment of the mission. After an elapsed time of about two minutes, the occulter-smallsat deploys the starshade petals, fully exposing the star trackers, sun sensors, and the thrusters to space. The deployment is a one-time event. After confirmation of starshade deployment and alignment verification, the motor is shut down for the remainder of the mission. The attitude determination and control system (ADCS) performs position and attitude determination. If the spacecraft is tumbling, the ADCS issues reaction wheel-based attitude control commands to de-tumble the spacecraft. Once the spacecraft has attained 3-axis stability, the occulter-smallsat orients the body-mounted solar panels toward the sun. The spacecraft communicates with the KSAT network of Ground Stations (the baselined NASA Near Earth Network asset for this study) via S-band to downlink its orbit and health status. Ground operators evaluate the data received and uplink updated spacecraft commands. The uplinked commands are stored in the spacecraft on-board computer memory for execution at specified times or conditions. Ground communication is a scheduled event and can occur only when the spacecraft have a line-of-sight to the ground station. The occulter-smallsat performs check-out tests by executing a series of commands to verify that all subsystems are performing per specification, including data transfer and communication to the ground as a part of the commissioning process. Successful demonstration of these verification tests, including its ability to (at a later time) communicate with the free-flying telescope-cubesat and to perform maneuvers, completes the commissioning process. The commissioning phase includes the calibration of the propulsion system on the occulter-smallsat.

Telescope-cubesat deployment and commissioning

After the mission control center has confirmed successful commissioning of the occulter-smallsat, it schedules the command sequence which will deploy the telescope-cubesat mainly in cross-track direction. Immediately after exiting the 6U dispenser, the telescope-cubesat generates power from its body-mounted solar panels. The deployable solar arrays are released after an elapsed time to minimize re-contact risk with the occulter-smallsat. After the ADCS has stabilized the spacecraft and battery top-off is complete, the telescope-cubesat conducts vehicle checkout to verify the functionalities of the subsystems. The telescope payload assembly, which includes its control electronics, camera, and the Thermal Electric Cooler (TEC), will perform a series of tests to verify that its science instruments are performing as specified. In addition, the telescope-cubesat performs crosslink communication with the occulter-smallsat by sending and receiving data at 220 kbps (i.e., maximum radio capability) in S-band. Through ground command, the telescope-cubesat will conduct target pointing to determine its pointing control accuracy.

Formation acquisition

After successful deployment of the telescope-cubesat, the occulter-smallsat performs a sequence of cross-track maneuvers such that after four weeks the two spacecraft build a cross-track separation of 500km at the nodes through a difference in right ascension of the ascending node. During this acquisition phase, both spacecraft

conduct crosslink communication tests to verify their S-band connectivity. Specifically, the occulter-smallsat receives raw GNSS measurements and navigation data from the telescope-cubesat, and the occulter-smallsat transmits its computed thruster firing times and durations to the telescope-cubesat in parallel. Additionally, the ground segment downloads captured images from the telescope and provides high-level guidance commands to both spacecraft to verify that the formation can align with a specified target with the required ±10cm accuracy. Successful demonstration of crosslink communication and formation alignment at the nominal separation certify that both spacecraft are ready to proceed to the nominal science phase.

Science

The majority of the mission lifetime is spent in the science phase, where target star observations are conducted while the spacecraft are in eclipse (see Figure 5). Science phase operations are divided into observation sequences and formation reconfigurations. Each observation sequence consists of a set of target star observations which are up to five minutes in duration and centered at the ascending or descending node (depending on LTAN). The number and duration of these observations is pre-computed and uploaded to the formation via telecommand. The planning process for each observation sequence accounts for the predicted durations of camera shutterings due to thruster firings. Between the target star observations, the occulter-smallsat performs a sequence of maneuvers to re-align the formation with the target star.

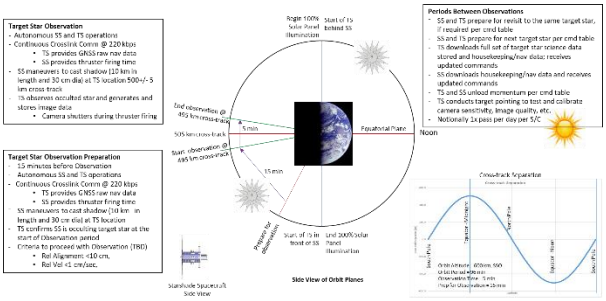

Figure 5: mDOT science phase. TS: telescope-cubesat. SS: occulter-smallsat.

The preparation of a target star observation takes about 15 minutes before the start of each observation. During this period, precise state estimates produced by the on-board Distributed multi-GNSS Timing and Localization (DiGiTaL) navigation system are used by the occulter-smallsat for precise formation alignment acquisition[8]. The deep shadow is 500km from the starshade along the line-of-sight (LOS), is 30cm in diameter (perpendicular to the LOS), and is 10km long (along the LOS). Additionally, the reaction wheels on the telescope-cubesat are used to align the boresight of the telescope with the target star and stabilize the attitude so that the tip/tilt mirror can stabilize the image in the science instrument.

During a target star observation, the telescope-cubesat continues transmitting raw GNSS measurements and navigation data to the occulter-smallsat for accurate relative navigation. The occulter-smallsat uses the state estimates from DiGiTaL to plan maneuvers using the radial and tangential thrusters to keep the telescope within the shadow produced by the starshade[8]. The starshade primarily maneuvers in the radial direction to counteract the relative acceleration perpendicular to the LOS between the spacecraft, thereby keeping the telescope inside the 30 cm diameter shadow. In parallel, the occulter-smallsat sends its computed thruster firing times to the telescope-cubesat for camera shuttering. This is required to avoid interference of plume flashes during observations.

At the conclusion of an observation sequence, the occulter-smallsat performs autonomous reconfiguration maneuvers to acquire the next scheduled target star in the command table. During these periods, the spacecraft download science and navigation data to the ground, de-saturate the reaction wheels using the magnetorquer rods, and conduct periodic camera calibrations. The process for preparing, conducting, and exiting target observations is repeated for each target star. mDOT is expected to observe at least 15 target stars during its mission life of 1.1 years. There is no driving science data latency requirement, so science data collection is opportunistically scheduled with KSAT, notionally at the conclusion of each observation sequence.

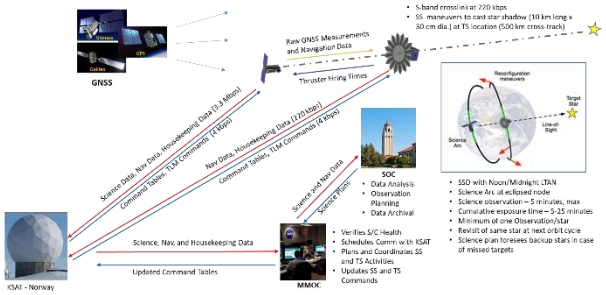

Figure 6: mDOT mission architecture. TS: telescope-cubesat. SS: occulter-smallsat.

Figure 6 illustrates the mDOT mission architecture. All activities performed by the spacecraft are planned and coordinated by the NASA's Multi-Mission Operations Center (MMOC), with inputs from the Science Operations Center (SOC), by uploading updated command tables to both spacecraft. The spacecraft execute these commands autonomously until the MMOC

intervenes or uploads new command tables. Both spacecraft receive GNSS signals from GPS, GLONASS, and Galileo constellations to generate their raw measurements and navigation data. The KSAT ground station in Norway serves as a link between the spacecraft and MMOC. Ground communication to downlink data and uplink updated commands is a coordinated event and is performed one spacecraft at a time. Stored image data and spacecraft health status data are transmitted to the Ground at 3.3 Mbps in S-band.

Decommissioning

At the end of the mission, ground control will issue final commands to the spacecraft. The telescope-cubesat is commanded to orient its solar panels in the velocity direction and the occulter-smallsat is commanded to orient the starshade in the velocity direction to maximize the effects of atmospheric drag, causing a gradual reentry. The occulter-smallsat is also commanded to perform a sequence of maneuvers once per orbit opposite to the velocity direction until the remaining propellant is depleted. This will decrease the perigee altitude of the spacecraft orbit, accelerating its reentry into the atmosphere. Both spacecraft are expected to burn in the atmosphere well before 25 years.

ORBIT DESIGN

The absolute orbit of the mDOT mission is sun-synchronous (98° inclination) with LTAN between 9AM-3PM or 9PM-3AM. This orbit was selected to ensure that one of the nodes is always in earth's shadow. Observations are performed at this node to ensure that the starshade is not illuminated by sunlight or earth albedo during observations, thereby minimizing the noise in images collected by the camera. Sun-synchronous orbits are also desirable for a wide range of earth observation missions, providing many launch opportunities. The nominal altitude of the orbit is 600 km to minimize the effects of differential drag on the formation while still allowing passive de-orbit within 25 years if the spacecraft maximize their area in the velocity direction at decommissioning. The requirements and nominal parameters for the orbit are provided in Table 5.

Table 5: mDOT absolute orbit.

Requirement	Limits	Nominal
Orbit altitude [km]	≥500	600
Eccentricity [-]	<0.02	0.001
Science mission duration [years]	≥1	1.1
LTAN [solar time]	9AM-3PM or 9PM-3AM	12AM

It was demonstrated by the authors that the delta-v cost of observing a target star using a formation in Earth's orbit can be reduced by only performing maneuvers to counteract the relative acceleration perpendicular to the LOS during observations, allowing the inter-spacecraft separation to passively drift[4,9]. The shadow produced by the starshade is long enough (10km) to enable observations up to 5 minutes in duration in low Earth orbit. The delta-v cost can be further reduced by ensuring that the formation is aligned primarily in the positive or negative cross-track direction when observations are performed such that the starshade and telescope orbits have equal semi-major axes. To maximize the number of targets mDOT can observe, the formation alignment is allowed to deviate by up to 10° in the (anti-)along-track direction during observations (see green cone in Figure 7). While increasing the separation in the along-track direction increases the delta-v cost of observing a target, this effect is mitigated by properly selecting the number and duration of observations[4]. Using this approach, the formation can be aligned with a science target with a specified right ascension and a declination in the range of -18° to +2° (Figure 7, left) or -2° to +18° (Figure 7, right) at any time, depending on the sign of the cross-track separation at the node in eclipse.

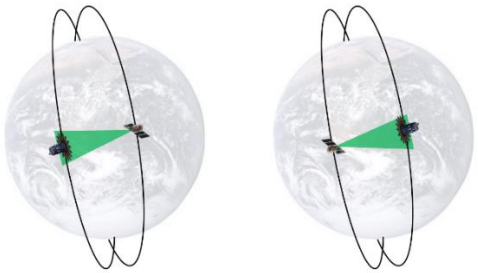

Figure 7: mDOT relative orbits for observing targets in the southern celestial hemisphere (left) and northern hemisphere (right). The observation cone is colored in green.

Because the RAAN of the absolute orbit drifts over time due to Earth's oblateness, the formation passively aligns with science targets with different right ascension. Accordingly, the delta-v cost of aligning the formation with a different target primarily depends on the difference in declination. With this in mind, Figure 8 shows the portions of the sky that can be imaged in science plans focusing on the northern hemisphere (red) and southern hemisphere (blue) including known targets of scientific interest.

There are sets of target stars in both the northern and southern hemispheres that satisfy the science objectives of the mission. It is hereafter assumed that the baseline mission uses the northern hemisphere science plan for simplicity. To minimize the delta-v cost of the mission, each target is observed when the pointing vector is as close as possible to the (anti-)cross-track direction, which also ensures that the orbits of both spacecraft have

the same semi-major axis. It follows that the relative orbit of the formation includes a 4° offset in RAAN with small differences in the mean anomaly and eccentricity vector. During each observation of a target, the inter-spacecraft separation passively drifts between 495km and 505km.

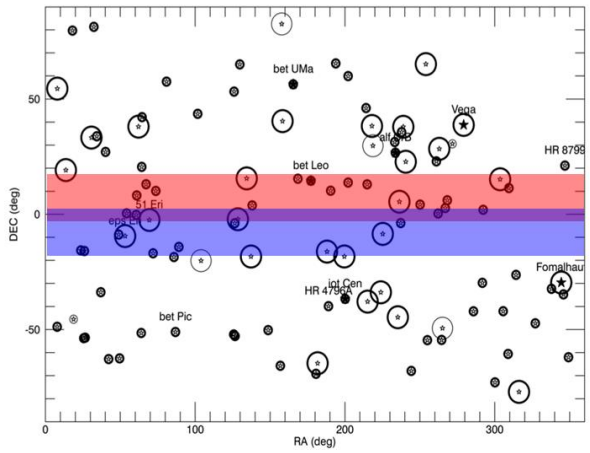

Figure 8: Candidate science targets for mDOT variants focusing on northern hemisphere (red) and southern hemisphere (blue).

Next, it is necessary to consider the safety of the formation. Passive collision avoidance can be ensured using the well-known relative eccentricity/inclination (e/i) vector separation technique[10]. Using this method, a user-specified separation in the plane perpendicular to the flight direction can be set by constraining the relative eccentricity and inclination vectors to be (anti-)parallel. Because the relative inclination vector (which includes the difference in RAAN) is so large for mDOT, it is evident that the point of closest approach is over the poles. Accordingly, it is sufficient to demonstrate that the magnitude of the relative eccentricity vector is larger than the expected difference in the semi-major axis of the orbits (≤2km including combined effects of maneuvers and precession of the absolute orbit over a 10-orbit observation sequence). To ensure a minimum separation of 1km, which is deemed sufficient to ensure passive safety in the event of an extended loss of maneuvering capability, it is necessary to ensure that the angle between the pointing vector to the target and the cross-track direction is at least 0.35°.

Figure 9 shows the evolution of the relative position in the radial/cross-track plane over one orbit for formations configured to observe targets with 0.35° (blue), 0.5° (red) and 1° (yellow) offsets in the (anti-)flight direction. It is evident from this plot that the minimum separation is 3km for the target with a 0.35° offset, which is sufficient to guarantee a 1km separation with the worst-case difference in the semi-major axis of the orbits. Increasing the along-track offset monotonically increases the minimum separation between the spacecraft.

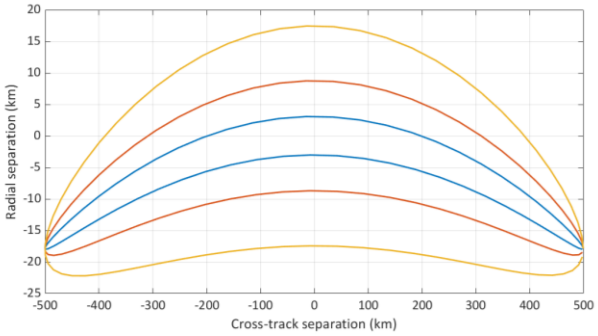

Figure 9: Evolution of relative position in radial/cross-track plane for one orbit following observations of targets with 0.35 (blue), 0.5 (red), and 1 (yellow) degree offsets in the (anti-)flight direction.

A conservative delta-v budget for the baseline mDOT mission is provided in Table 6 including a margin of 25%. It was validated by conducting high-fidelity simulations of the mission for the science targets described in Table 7. These simulations include 3-sigma navigation errors, dynamics modeling errors, and maneuver execution errors consistent with the performance of the DiGiTaL navigation system and foreseen green-propellant thrusters (ECAPS)[8,11,12]. The control logic used in these simulations is described in detail in a previous work by the authors[4].

Table 6: mDOT mission delta-v budget.

Allocation	Δv [m/s]	Burn duration [min]
Formation Acquisition	275	107
Science Phase	400	133
Safe Modes	25	8
De-Orbit	50	16
Margin (25%)	190	-
Total delta-v	940	264

Table 7: mDOT science targets and delta-v.

Target star	Observations [m/s]	Reconfigurations	
		Same target	Different target
alf CMi	11.6	3.7	13.2
16Zet Hya	24.4	22.1	33.2
70 The Leo	13.0	3.3	17.0
Beta Leo	3.2	0.0	15.4
HD 107146	34.8	21.2	28.7

50 Gam Aql	34.4	21.2	7.6
alpha Aql	4.8	1.8	14.1
HD 15115	4.0	0.6	10.5
29 Tau	4.3	0.8	8.0
1 Ori	8.7	5.7	3.2
HD 32297	8.1	6.0	4.7
24 Gam Ori	1.8	0.0	5.1
58 Alp Ori	0.9	0.0	-

FLIGHT SYSTEM CAPABILITIES

Launch Vehicle Compatibility

mDOT requires an ESPA Grande support structure on a launch vehicle with a 5m fairing or larger. The mDOT team will need to coordinate with the launch vehicle provider to ensure the mDOT design meets the launch environment of the selected launch vehicle, but the team expects that the Atlas V, Delta IV, or Falcon 9 could be configured to satisfy the necessary launch envelope. With the exception of the telescope-cubesat dispenser and rear thruster protruding through the interface ring and into the interior of the ESPA Grande, the occulter-smallsat conforms to the ESPA Grande secondary payload envelope of 1.0m high x 1.1m wide x 1.4m long, measured from the ESPA Grande 24-inch ring interface. The 1.4 m length limit corresponds to a 5 m fairing. The ESPA User's Guide (November 2018) states that auxiliary payloads are allowed to take advantage of the ESPA internal volume, if this volume is not occupied by a propulsion system or other mission element[13]. Assuming an ESPA with no internal elements, mDOT would be allocated a "pie slice" of the internal volume. The allocation of the ESPA internal volume should be confirmed by the launch vehicle provider and/or the mission integrator once the mission integrated payload stack is defined. As the design is refined, optimization can include recessing the 6U dispenser partially into the occulter-smallsat body to reduce the protrusion into the ESPA internal volume. This would shift the propellant tank location away from the ESPA interface, so management of the center of mass location would be the limiting factor. In the event that ESPA internal volume is not made available to auxiliary payloads, the size of the propellant tank would need to be reduced to make room for the dispenser within the body, with a corresponding impact to propellant budget and science observation time.

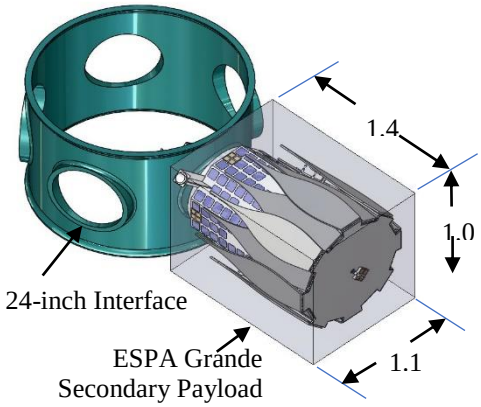

Figure 10: The stowed occulter-smallsat fits within the ESPA Grande volume allocation.

The occulter-smallsat will be deployed from the ESPA Grande using a 24-inch separation ring (Planetary Systems Inc. Lightband or similar). The current ESPA allocation for mDOT mass is 320kg. The ESPA 24-inch port is rated for up to 465 kg when the center of mass is located within 50.8 cm (20 inches) from the ring interface. Figure 10, Figure 11, and Figure 12 illustrate the compatibility of the mDOT design with the ESPA Grande ring.

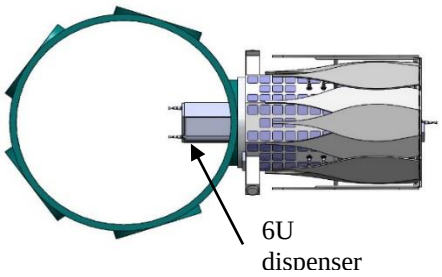

Figure 11: The telescope-cubesat dispenser protrudes into the ESPA Grande interior.

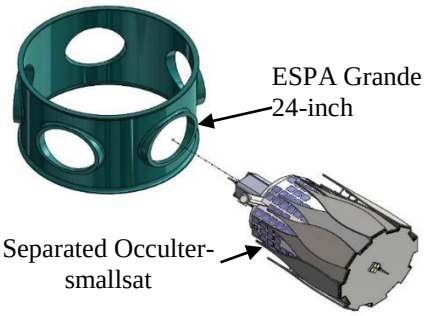

Figure 12: Springs in the separation ring send the occulter-smallsat to a safe distance before deployment of the starshade.

Occulter-smallsat

The occulter-smallsat consists of a small spacecraft with approximately 1.0m x 1.4m x 1.1m octagonal structure which provides support to the 16-petal starshade. The starshade is 3m in diameter with petals manufactured to within 0.1mm pattern shape tolerance. The starshade is stowed during launch and deployed like an umbrella by a motor after the occulter-smallsat has been ejected from the ESPA Grande. The telescope-cubesat is carried inside a 6U ISIS DuoPack CubeSat Deployer mounted at the opposite end of the occulter-smallsat. Eleven (11) 5N green propellant thrusters are arranged in pairs, plus one single on the starshade, to provide radial, tangential, and normal velocity control independent from spacecraft attitude.

Table 8: Occulter-smallsat subsystems.

Subsystem	Components	TRL
Payload	Starshade hub with 16 deployable petals; Starshade deployment motor; Snubbers (from Tendeg)	5
Structure	Aluminum Primary Structure; ISIS DuoPack CubeSat Deployer; Planetary Systems Standard Lightband of 24 inch diameter	7-9
C&DH	Tyvak SBC with Tyvak Linux BSP Operating System; ARM Cortex A8+ DSP Coprocessor; 512 MB RAM; NAND-Flash 8 GB SD-card	9
Electrical Power	Body-mounted UTJ Solar Cells (from Spectrolab); LG INR 18650HG2 300mAh Battery Cells (32 cells); EPS Stack with BioSentinel legacy	9
Comm	Two (2x) Cesium SDR; S-band with Tx/Rx Module (TRM) – Primary and Redundant; 4x S-band patch antennas (2 for crosslink, 2 for downlink/TT&C) – Primary and redundant	5-6
ADCS	BCT Nano Star Trackers (2x); BCT MICD Coarse Sun Sensors (2x); BCT RW4 Reaction Wheels (4x); Microcosm MT-140 Magnetorquer Rods (3x); BCT XACT Gen3 ADCS Processor	9
GNC	Guidance, Navigation, and Control software, including DiGiTaL[8] (developed by Stanford)	5
Thermal	Combination of active and passive control with allocation for heaters, MLI, and temperature sensors	8
Propulsion	11x 5N HPGP Thrusters (from Bradford, ECAPS); LMP-103S Green Propellant; 77.9L (propellant load volume); Propellant Tank from ATK	5-9
Flight Software	cFE/cFS, Blue Canyon (XACT)	8

Two pairs of thrusters are used for radial velocity adjustment, two pairs for tangential, and a pair and single thrusters for normal velocity adjustments. Placement and orientation of the radial and tangential thrusters were selected to minimize plume impingement onto the petals while also minimizing rotational torques due to the shifting of spacecraft center of mass over time. Solar cells and six Cesium patch antennas populate the spacecraft body panels. One crosslink patch antenna is mounted on the starshade hub and one on the opposite panel. Two vertical structures pointing in opposite directions, designed to be out of view of the telescope-cubesat during observations, provide support to the GNSS antennas. Occulter-smallsat avionics, including propellant tanks and batteries, are located as opposite to the starshade in the spacecraft as possible. This helps to balance the spacecraft (center of mass near geometrical center) as well as to minimize plume impingement of radial and tangential thrusters on the petal edges.

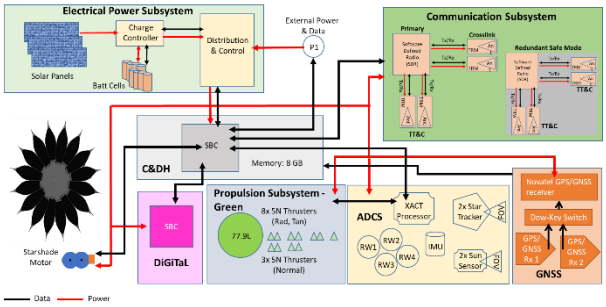

Figure 13: Occulter-smallsat functional block diagram.

Table 8 provides a summary of the major subsystem components of the occulter-smallsat, including the assessed Technological Readiness Level (TRL). When components of the subsystem have different TRL, a range of TRL is provided. In particular, the payload, communication, GNC, and propulsion subsystems have components with TRL<6 which need a dedicated technology maturation plan for mission implementation. Figure 13 shows the functional block diagram of the occulter-smallsat. Table 9 lists the key technical flight system margins for the occulter-smallsat, excluding the telescope-cubesat. The margin is computed by subtracting Current Best Estimate (CBE) from allocation and dividing by allocation.

Table 9: mDOT occulter-smallsat margins

Resource	CBE	Allocation	Margin
Dry Mass [kg]	138	---	---
Prop Mass [kg] (81.2kg for delta-V)	96	---	---
Lift-off Mass [kg] Incl. telescope-cubesat	246	320	23%
Solar Power (W) - EOL	177	37	>100%
Battery Power (Wh)	345.6	187	85%

Battery DOD (%)	19.2	80	60.8
Relative Position Nav Accuracy (RMS)	2 cm (3D)	6 cm (R, T); 1km N	66% >100%
Relative Position Ctrl Accuracy (MAX)	10 cm (R,T)	15 cm (R, T)	33%
Pointing Control Accuracy (deg)	0.002	1.00	>100%
Pointing Knowledge Accuracy (deg)	0.002	1.00	>100%
Slew Rate (deg/s)	0.125	>0.063	98%

The occulter-smallsat is sized for mounting to an ESPA Grande. The main components of the spacecraft are shown in Figure 14 and Figure 15. The main body of the spacecraft is an octagonal structure, 70cm across. This is large enough to mount on a 24-inch separation ring while small enough to allow the 3m-diameter starshade structure to fold over the octagonal body without exceeding the ESPA Grande volume constraints. The spacecraft body and internal support structure are constructed primarily of aluminum (subject to change with refined thermal analysis). Each face of the octagonal body is covered with 35 solar cells. Once the starshade is deployed, the body-mounted panels are exposed to the sun and are sufficient to meet power needs.

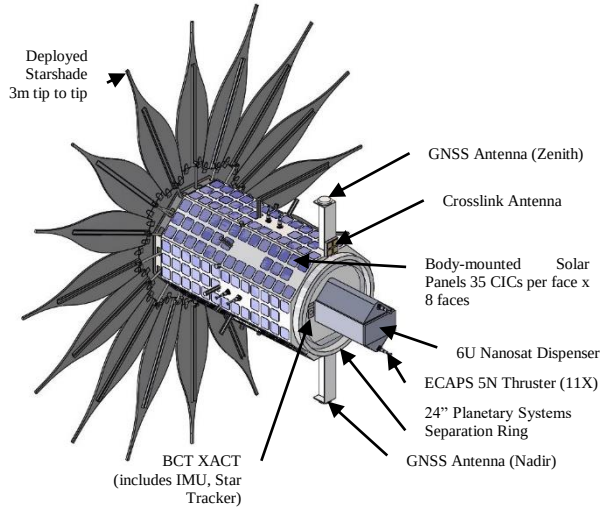

Figure 14: Rear view of occulter-smallsat.

Pairs of 5N thrusters are mounted on the +/- axes to allow for 3-axis translational control. The face of the starshade is the only surface with a single 5N thruster. The thrusters are located such that a net thrust is provided through the center of mass (for the deployed configuration). The 91-liter fuel tank (77.9L fill capacity) is located along the axis of the octagonal body. The tank carries 96kg of available ADN green propellant (LMP-103S) at launch, of which 81kg is usable for delta-v. The 6U NanoSat dispenser is mounted opposite of the starshade and protrudes through the 24-inch separation ring. A pair of 5N thrusters straddle the dispenser. The location of the dispenser along the main axis of the spacecraft ensures that release of the telescope-cubesat will have minimal impact on the center of mass of the occulter-smallsat and will minimize tumble at release.

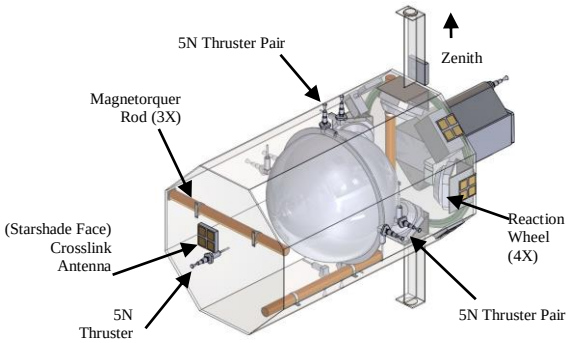

Figure 15: Internal view of occulter-smallsat.

Two star trackers are positioned with orthogonal fields of view. One looks along the main spacecraft axis. The dispenser shades the star tracker from the thruster flare. This star tracker could also be located on the face of the starshade with similar performance. The other star tracker is mounted in one of the upper octagonal faces. Four reaction wheels are located within the spacecraft against the 24-inch interface plate. They are oriented along tetrahedral axes, providing 3-axis attitude control with redundancy. Three 68cm-long magnetorquer rods are placed orthogonally as available volume allows. The radios, power system, and computer are located close to the interface plate and positioned to keep the center of mass within 2cm of the body axis. The center of mass is within 51cm of the 24-inch ESPA interface in the launch configuration. Patch antennas are located on the face of the starshade, on the dispenser end of the occulter-smallsat, and on the two lower octagonal faces, 45 degrees off nadir. Four additional patch antennas are mounted to four of the unoccupied faces and connected to a separate Cesium radio for redundancy. Two GNSS antennas are located on extension arms in the zenith and nadir directions. The extensions are intended to maximize the antennae's field of view (allowing for 120 degrees FoV) unobstructed by the large starshade.

The starshade design consists of 16 deployable precision petals which are mounted onto a structural base deck. The deck structure is the mounting plate for the petal hinges, the petal central deployer mechanism, and the precision structural interface to the aft end of the bus. When the petals are stowed, they fold up parallel to the bus central axis. The petals are seated in cup/slotted cone devices onto 16 posts with brackets that are integrated into the bus and restrained. A resettable launch

restraint/release device is mounted to the end of the post. Releasing this device disengages the petals so that they can be deployed to their final position by the deck mounted deployment mechanism rotating its linkage arms that connect this mechanism to the individual petals. The petals are rotated down and locked out in this position through tapered pin engagements at the hub. Details of the starshade's overall mechanical design, including deck, petals, hub, linkage arm, and petal launch restraint are available but omitted for brevity. Figure 16 shows the starshade designed for mDOT by Tendeg[14].

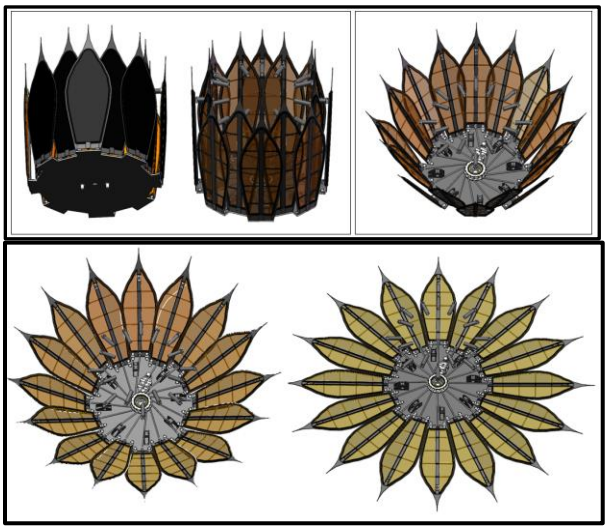

Figure 16: mDOT's starshade stowed configuration (top-left), first motion (top-right), and deploying to final configuration (bottom).

The propulsion system must be selected to satisfy five requirements. First, the thrust must be sufficient to keep the formation aligned with each of the target stars. Second, the duty cycle of the thrusters should be kept under 50% to minimize the duration of camera shuttering during observations. For the baseline science plan, it was found that a thrust of 10N is sufficient to control the formation with short thruster firings (<5 seconds). Third, the propulsion system should have the largest possible specific impulse to meet the delta-v requirement for the mission with reasonable propellant mass (<100kg). This results in a minimum specific impulse of 220s. Fourth, the starshade spacecraft must be able to generate thrust in any direction without performing an attitude maneuver to ensure that the formation can controlled during observations with the starshade facing the target star. Finally, the propulsion system must generate thrusts that act through the center of mass of the spacecraft to minimize the momentum accumulated in the reaction wheels during observations. To meet these requirements, the selected propulsion system consists of a set of 11 5N high-performance green propellant thrusters from Bradford ECAPS[11,12]. These thrusters have a specific impulsive of 240s, and a density 24% higher than hydrazine.

The thrusters are positioned to provide torque-free translation maneuvers at all times during the mission accounting for the shifts in the center of mass due to propellant expenditure. The thrusters are aligned in the positive/negative direction of each of the principal axes. Reaction wheels can compensate for undesired torque generated from misalignment of thruster nozzles and provide for control in the event of a malfunctioning nozzle pair. The thruster arrangement provides 10N thrust per axis in the plane perpendicular to the line of sight during observations, meeting the thrust requirement for the mission. The sizing of ADCS hardware is based on the mission design, spacecraft body design, sun-synchronous orbit environments, and corresponding constants (e.g. sunlit area, gravity constant, magnetic constant, solar reflection factor, drag coefficients, atmospheric density). The ADCS system components are provided in Table 10.

Table 10: mDOT occulter-smallsat ADCS system components

Component	Vendor	Mass [kg]
Star tracker (x2)	BCT star tracker	0.35
Coarse Sun sensor (x2)	BCT MICD, Strip Assembly	0.008
Reaction wheels (x4)	BCT RW4	12.0
Magnetorquer Rod (x3)	Microcosm MT-140	15.9

The occulter-smallsat employs one communication system for both crosslink and telemetry, tracking and command (TT&C), as shown in Figure 17. It also includes a dedicated redundant system for emergency and safe mode TT&C based on the same hardware solution as the primary system. The nominal system works in S-Band and provides both TT&C, emergency and safe mode TT&C, and crosslink communication with the telescope-cubesat to exchange raw GNSS measurements, thruster firing times, and auxiliary data. The telescope-cubesat employs the same hardware solution for the crosslink and science data downlink, while the bus provides TT&C and redundant science data downlink capability. mDOT plans to use the KSAT ground station network (NEN) and the SG1 dish is the baseline for the link analysis. Initial analysis show that mDOT closes both the TT&C and Science data RF downlink with >> 6 dB. The crosslink between the spacecraft closes with 5.5 dB at max expected distance of 510 km. In addition, the mDOT team also performed preliminary link analysis using the KSATLite ground stations, which consists of 3.7 m dishes (versus the 11.3 m of SG1) co-located with traditional KSAT dishes. While these results indicate that KSATLite assets may

meet mDOT requirements, KSATLite is not integrated with NASA NEN, therefore a future trade will be performed to assess the use of KSAT vs KSATLite assets based upon cost, performance, and operational complexity.

From the MTM, the data volume of science data that needs to be downloaded after each observation varies from 10 MB to 600 MB. Initial analysis shows that a 3.3 Mbps data rate allows all science data generated in one observation to be downlinked to a ground station in 1 to 5 passes. mDOT has ~ 14 daily available passes with SG1. The bandwidth occupancy is estimated to be within the 5 MHz bandwidth limit.

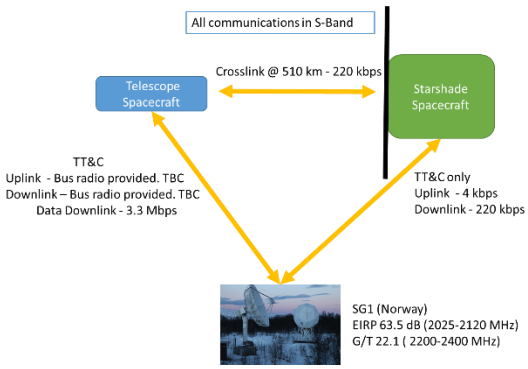

Figure 17: mDOT's radio communication links.

The electrical power subsystem (EPS) was analyzed by operational mode. The most demanding mode is found to be during a science observation. The remaining modes were assessed to be less demanding than observations. For analysis, the LTAN noon/midnight orbit was assessed, which is a worst case for power considerations. For this mode the spacecraft uses body-mounted solar cells capable of generating at least 192W (assuming Peak Power Tracking) of power at end-of-life (EOL); 345 Wh of battery storage capacity at EOL is provided. Spectrolab provides solar cells which will be installed onto the exterior of the spacecraft body, 35 cells per surface (8 sides - 280 total cells). This solution allows for pointing in all directions while still receiving adequate power while in sun. The panels are equipped with UTJ solar cells with proven 28.3% efficiency. The occulter-smallsat uses 32x LG INR 18650HG2 3000 mAh Li-ion batteries, with four series and eight parallel connectivity. The maximum depth-of-discharge (DOD) is 20% due to the LEO orbit selected, as the orbit cycle count is < 6,500 for the entire 1.1-year mission; future refinement of the number of charge/discharge cycles could allow for a less-conservative DOD.

The EPS boards leverage the design used on BioSentinel, which is a mission of NASA Ames Research Center mission scheduled to launch in 2020 on EM-1[15]. The power management card controls solar arrays, monitors over current, and manages battery usage. The power distribution card is a switch board that controls power switching, DC-DC conversion, and power regulation, among others. The EPS must supply 12V bus voltage and 3.3V of regulated voltage. Additionally, each of the batteries in series has an individual management card. For the current battery design, there are eight parallel battery strings; thus, eight battery management cards.

Formation Guidance, Navigation, Control (GN&C)

A precise relative navigation system is required to: 1) estimate the absolute orbit of the occulter-smallsat, and 2) estimate the relative position and velocity of the telescope-cubesat with respect to the occulter-smallsat. These functionalities can be accomplished by the Stanford's DiGiTaL system which includes a hardware layer (GNSS receiver, antennas, RF peripherals) and a software layer[8].

The baseline receiver is from the Novatel OEM-7 dual frequency GNSS receiver series. This is one of the most well-known receivers for cubesats and smallsats such as CanX-2 and E-POP. Novatel OEM 7 offers dual frequency tracking capability to estimate/mitigate the ionospheric path delays for long-baseline precise positioning in the LEO environment. This sensor provides carrier-phase measurements with millimeter-level noise, enabling estimation and filtering algorithms to provide relative state estimates with 2cm accuracy (3D, rms).

To ensure continuity and robustness of GNSS measurements, the both spacecraft are equipped with two GNSS antennas mounted on extension arms on the zenith and nadir faces of the spacecraft bus to ensure than each antenna has an unobstructed 120deg FoV. Only the most zenith-pointing antenna is used for navigation purposes at any time. The antenna selection is done through an RF switch based on attitude information provided by the spacecraft bus. This allows support of ADCS safe mode and tumbling operations.

Because the absolute orbit knowledge requirements are benign, the absolute orbit is estimated directly from the position and velocity solutions from the GNSS receiver. Instead, the pseudocode and carrier-phase measurements from both spacecraft (transmitted using the crosslink) are used by the DiGiTaL software to compute relative state estimates in real time with accuracy of 2cm or better (3D, rms). This is accomplished using differential carrier-phase techniques similar to those used on the PRISMA mission[16]. While carrier-phase measurements have millimeter-level noise, they are subject to an integer offset in the number of cycles. This offset must be computed for each measurement using integer ambiguity

resolution (IAR). To meet the relative navigation requirements for mDOT, this must be accomplished onboard in real-time. To minimize the computation effort required for this task, DiGiTaL computes wide-line measurement types by fusing carrier-phase measurements from different frequencies and constellations (e.g. Galileo, GLONASS, Beidou). These measurement types benefit from common error cancellation (e.g. ionosphere offset) and reduce the search space for IAR. Figure 18 shows the state estimation error and formal 3-sigma covariance for the filter after activation of IAR as obtained through hardware-in-the-loop tests at Stanford[8].

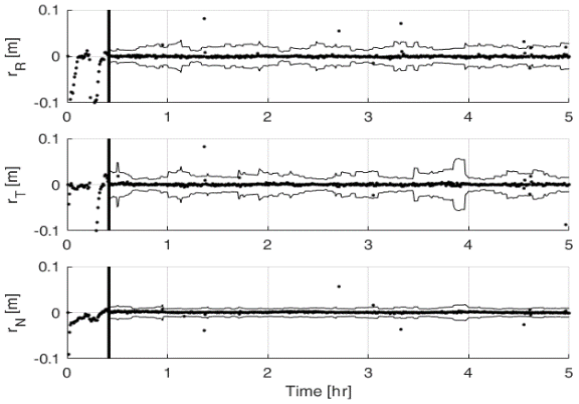

Figure 18: Estimation error and 3-sigma formal covariance for DiGiTaL relative position estimates after IAR fix (vertical black line).

The absolute and relative state estimates provided by DiGiTaL are used by the GN&C algorithms to compute the translational maneuvers required to control the formation. Formation control is divided into two distinct modes: 1) observation mode, and 2) reconfiguration mode. Transitions between these modes are deterministically computed from the properties of observation sequences uploaded from the ground.

In observation mode, a closed-form state-space control logic is employed that simultaneously minimizes the number of executed maneuvers and minimizes propellant consumption. The number of maneuvers is minimized by planning the maneuvers such that the relative position in the plane perpendicular to the LOS crosses the full diameter of the shadow. These maneuvers act in direct opposition to the relative acceleration perpendicular to the LOS, ensuring that the formation is efficiently controlled. An example trajectory of the relative position in the plane perpendicular to the LOS is shown in Figure 19. This trajectory corresponds to the first in a sequence of ten observations of a target, resulting in a large relative acceleration in the plane perpendicular to the LOS and a cumulative delta-v cost of 3 m/s for the five-minute observation. This trajectory includes 36 maneuvers with burn times ranging from 0.2 to 3.3 seconds. Because the maneuvers are planned in closed-form, this control logic runs in less than 1s on the Tyvak processor baselined for the occulter-smallsat.

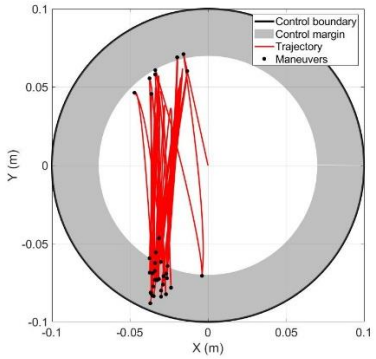

Figure 19: Trajectory of telescope (red) in plane perpendicular to LOS during observation mode with control boundary (black), margin (gray), and maneuver locations (circles).

In reconfiguration mode, a stochastic model predictive controller is used to plan a maneuver sequence that ensures that the formation is aligned with the target at the start of the next observation. This control logic is the same for reconfigurations to re-align with the same target or to align the formation with a different target. At each update step (10 minutes or slower), the state estimate and covariance are propagated to the start of the next observation by numerical integration of the equations of motion including dominant perturbations in LEO and any previously planned maneuvers. If the desired state is within the 3-sigma covariance bound of the propagated state or the entire 3-sigma covariance bound is within the control window, the previous maneuver plan is kept and planned maneuvers are executed until the next update. If neither of these conditions is satisfied, the maneuver plan is updated using a recently developed globally optimal impulsive maneuver planning algorithm[17,18]. This is accomplished by first propagating the orbits of both spacecraft without any maneuvers. Next, the desired state of the occulter-smallsat is computed by adding the nominal relative state at the start of an observation to the propagated orbit of the telescope-cubesat. Finally, a maneuver sequence that drives the occulter-smallsat from the propagated state to the desired state is computed using the numerical maneuver planning algorithm[17,18]. Preliminary tests have found that this algorithm can be executed in less than 10s on the Tyvak processor baselined for occulter-smallsat. To enable observations to be performed over consecutive orbits, maneuver planning and execution are run autonomously on-board.

Navigation and control data is downloaded to the ground in regular intervals for post-facto analysis. A block diagram of the communication architecture for GN&C purposes is shown in Figure 20.

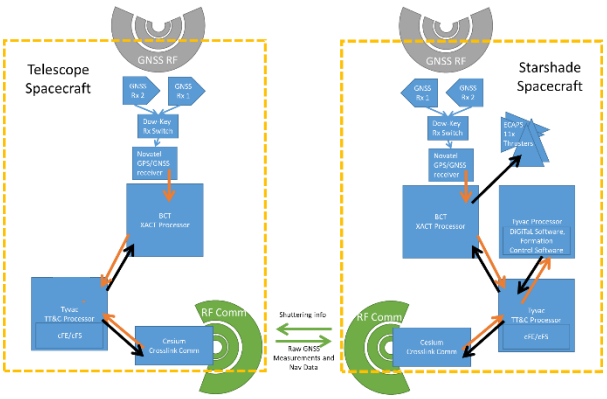

Figure 20: Communication flowchart for occulter-smallsat (left) and telescope-cubesat (right).

Telescope-cubesat

The telescope-cubesat is a 6U CubeSat that is carried and deployed by the occulter-smallsat. Blue Canyon Technologies (BCT) was contacted by the study team and provided a cost estimate for a LEO spacecraft bus which meets the top level mission requirements. Several options are available including the 21ASM1950 (BCT structure with simplified avionics), the BCT 6U RAVAN bus (with simplified assembly), or the FlexBus 6U platform which all meet the mDOT mission needs. In particular, the requirements on the telescope-cubesat bus are well within reasonable limits for current LEO CubeSat capabilities, and so procurement of a suitable bus is considered a low-risk item by the study team.

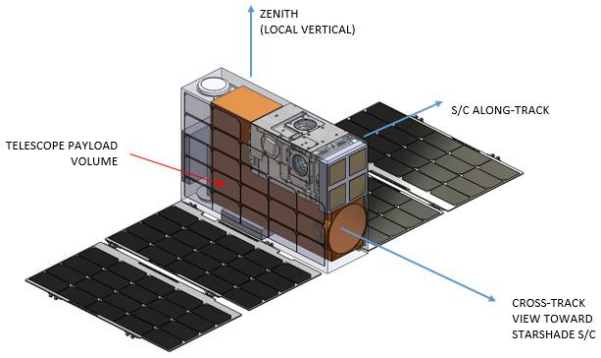

Figure 21: Isometric view of telescope-cubesat bus.

The telescope-cubesat has no propulsion system, thus it relies on its ADCS reaction wheels for attitude control and the magnetorquers for wheel desaturation. The telescope assembly occupies 4U volume in an L-shape configuration (see Figure 21 and Figure 22) which leaves 2U volume for housing spacecraft avionics. Solar cells are body-mounted on the spacecraft sun-facing panels and are augmented by deployable solar panels. Crosslink patch antennas are mounted on the aperture side and on the anti-aperture side. A patch antenna is mounted on the Earth-facing panel for DTE using NEN (KSAT). Similar to the occulter-smallsat, the telescope-cubesat is equipped with the DiGiTaL system for precise relative orbit determination. Data volume sufficient for three target stars is provided, including 600 MB per observation and two revisits per target, although data is intended to be downlinked after all target observations.

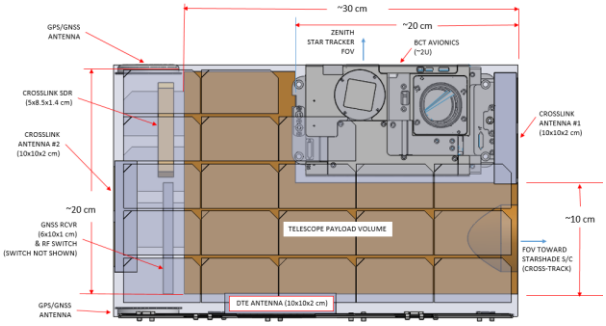

Figure 22: Dimensions of telescope-cubesat bus.

Table 11: mDOT telescope-cubesat resources.

Resource	Value	Note
Volume for telescope	4U in L-shape	See Figure 21 and Figure 22
DiGiTaL antenna	2x GNSS antennas, 1x GNSS receiver, 1 RF switch	GNSS antennas on Zenith and Nadir
Crosslink radio system	1 SDR, 3 antennas	SDR: 5x8.5x1.4 cm Each Antenna: 10x10x2cm
Payload power	45W in eclipse (15 minutes/orbit), 10W daylight	Duty Cycle for Science Observations
Pointing accuracy	±0.45deg, all axes	Capability of bus is ~0.007 deg
Design lifetime	18 months	Nominal mission duration 1.1 years
Orbit	600km altitude, 98deg inclination	LTAN: noon-midnight
Propulsion	None needed	
Science data volume	4 GB	Half of an 8GB SD card for science data.

Figure 21 and Figure 22 show the mechanical layout of the telescope-cubesat, while Table 11 and Table 12 list the flight system resources and major subsystem components. The overall system TRL has been assessed at 7-8 after accounting for payload interface modifications.

Table 12: Telescope-cubesat subsystems.

Subsystem	Components	TRL
Payload	Telescope assembly with 2 cameras, tip/tilt mirror, and TEC	7-8
Structure	6U from BCT; Telescope assembly to occupy 4U in L-shape form	
C&DH	Tyvak SBC with Tyvak Linux BSP Operating System; ARM Cortex A8+ DSP Coprocessor; 512 MB RAM; NAND-Flash 8 GB SD-card	
Electrical Power	BCT EPS	
Comm	Cesium SDR S-band with Tx/Rx Module (TRM); 3 S-band patch antennas (2 for crosslink, 1 for downlink); Xilinx FPGA host	
ADCS	BCT XACT	
Propulsion	None	
Flight Software	BCT, DiGiTaL	

The 6U telescope-cubesat plans to use a Cesium S-Band system to support TT&C and science data downlink with KSAT, downlink to the occulter-smallsat of GNSS data and uplink from the occulter-smallsat of camera shuttering information. The Cesium telecommunication system uses the same hardware configuration for both spacecraft. The bus TT&C capabilities provide redundant science downlink capabilities with KSAT.

TECHNOLOGY GAPS AND RISKS

System Engineering

mDOT's Project System Engineer (PSE) serves as the technical authority through all mission phases and chairs the Systems Engineering Team (SET). The SET manages the SE effort, including developing requirements, interface control documents (ICDs), verification and validation plan, tracking technical performance measures (TPMs), and performing trade studies and analysis. Payload-to-spacecraft ICDs are defined in Phase A, allowing independent testing of the instrument and spacecraft prior to integration. The Spacecraft-to-host ICD is defined early in Phase B to establish critical interfaces with the host spacecraft. Lower-level ICDs are developed as needed between critical hardware and software elements to ensure compatibility prior to integration. The mDOT's spacecraft team implements the spacecraft design using off-the-shelf components and systems wherever possible. The mission environments, both external and internal, are characterized to ensure that adequate design margins are incorporated for radiation effects, electrical system grounding and noise, and electromagnetic control for both on-orbit and launch environments.

mDOT's SET implements the mission science requirements identified in the science traceability matrix (STM). The instrument and mission requirements listed in the STM flow down to requirements on flight and ground segments as shown in the MTM (Table 1). The mission requirements in the MTM are used to derive mission system specifications and ICDs, particularly the payload-to-spacecraft ICDs. The Dynamic Object Oriented Requirement System (DOORS) tool is used for requirements tracking, flow-down, documentation, and verification. The instrument concept proposed by mDOT is modeled to validate that the technical performance meet the science objectives. Science constraints on the operations concept have been included to ensure that the science operations produce the required measurements. Throughout the formulation, implementation and development phases, the mission architecture, operations concept, and models will be cross validated to ensure consistency in meeting mission requirements.

Risk Assessment

The mDOT's risk matrix is illustrated in Table 13. It provides a snapshot of the main identified risks including a quantification of their likelihood and impact to the overall mission.

Table 13: mDOT 5x5 risk matrix.

Likelihood						
>80%	5					
<80%	4					
<60%	3					
<40%	2			**2,4**	**1**	
<20%	1	**12**		**3,10,11**		**5,6,7**
		1	2	3	4	5

Consequence

A summary of the risk assessment is provided in the following bullet list where risks IDs refer to Table 13.

1. *Starshade Deployment Failure*. Given that the starshade mechanism is a new design, there is a probability of incomplete deployment, adversely impacting science capability. *Mitigations*: Design a test system for deployment in 1g-environment to facilitate verification of the flight configuration. If the motor senses partial deployment, it stops and switches to a standby mode and waits for ground command for corrective actions.
2. *DiGiTaL/GN&C Computer Failure*. If the DiGiTaL/GN&C computer goes into Safe Mode (locks up) for more than 5 minutes, estimation and control accuracies are degraded, which can result in

missed or shorter observations. *Mitigations*: Include contingencies in science plan that re-allocate delta-v to other targets after control is re-established. Include redundant on-board computer.

3. *Propellant Quantity*. Since orbit maneuvers are required to align the formation with each target, there is a possibility that the loaded propellant may get depleted early, which can result in not achieving all mission objectives. *Mitigations*: Maximize propellant tank size and fill to capacity. Reduce occulter-smallsat mass. Include contingencies in science plan to account for deviations from predicted propellant expenditure.
4. *Solar Array/ Instrument Contamination by Thruster Plume*. Given that condensation of exhaust products or heat effects forms on solar arrays and instrument surfaces, there is a possibility that solar array efficiency and sensor readings will be degraded, which can result in reduced mission life and compromised mission data. *Mitigations*: Conduct plume impingement analysis. Investigate different propellant options and pick solution with acceptable thrust performance and minimal contamination impact. If possible, orient sensitive solar array and instrument surfaces away from thrusters.
5. *Telescope-cubesat Deployment Failure.* Given that the telescope-cubesat is deployed from a 6U Dispenser, there is a possibility that it will not deploy or will re-contact with the occulter-smallsat, which can result in mission loss. Mitigations: Verification of Dispenser using mass simulator during integration and testing. Verification of final installation. Ensure through analysis that Dispenser system provides sufficient delta-v to avoid re-contact.
6. *Re-contact with ESPA Grande*. Given that the occulter-smallsat will be ejected from the ESPA Grande, there is a possibility that the spacecraft could re-contact with the ESPA Grande, which can result in loss of mission (and orbital debris). *Mitigations*: Coordination with launch provider and analysis to determine appropriate wait time prior to spacecraft deployment and spacecraft power-up.
7. *Conjunction/ Collision between spacecraft.* Given that the minimum separation between the spacecraft occurs over the poles, there is a possibility that loss of nominal control on either spacecraft could cause a collision, resulting in loss of mission (and orbital debris). *Mitigations*: Exclude science targets with declinations within 0.35deg of ±8deg, ensuring passive collision avoidance via relative e/i-vector separation[10]. In the event of an extended navigation outage, the ground segment can command the occulter-smallsat to perform collision avoidance maneuvers.
8. *Telescope-cubesat Orbit Decay*. Given that the telescope-cubesat has no propulsion system, there's a possibility that the spacecraft may remain in orbit beyond 25 years after launch, resulting in non-compliance with the NASA Handbook for Limiting Orbital Debris (and International Standards). *Mitigations*: At the end of mission life, orient the spacecraft such that its largest surface area faces into the velocity vector to increase atmospheric drag forces.
9. *Rideshare Opportunity*. Given that the occulter-smallsat volume protrudes into the interior of the ESPA Grande ring, there is a possibility that a rideshare opportunity will not be available, resulting in a schedule slip while awaiting a suitable launch accommodation. *Mitigations*: Early negotiation and coordination with the launch services provider to ensure early identification of options will minimize overall impacts on project schedule.
10. *Starshade tolerance.* Given that the starshade must be accurately manufactured (0.1mm edge shape tolerance) and deployed, there is a possibility it cannot maintain the required tolerance under operational environment, which can result in image data contamination. *Mitigations*: Extreme care in selecting materials, machining of parts, and testing of assembly under similar operational environment.
11. *Plume Impingement*. Given that plume impingement on the starshade occurs during an observation, there is a possibility that exhaust gas degrades the shape of the petals over the mission, which can result in image data contamination. *Mitigations*: Tilt the R/T thrusters away from the starshade and use the reaction wheels to compensate for the thruster-induced torque. Design the occulter-smallsat to have its center of mass and R/T thrusters as far away from the starshade as possible.
12. *Cesium SDR & TRM Hardware at TRL 6.* Given that the Cesium radio hardware is not flight qualified yet, there is a possibility that it will not pass qualification testing before it is required for integration and testing. *Mitigations*: Keep updates on incoming qualification testing (planned for May 2019) and conduct trade study for alternative communication systems.

Technology Gaps

Most subsystems required for mDOT are currently at TRL 7 or higher (see Table 8 and Table 12 listing the spacecraft components). It is believed that all subsystems at lower TRL can be matured to TRL 6 or higher within two years through qualification testing on-ground and flight demonstrations on upcoming missions. Current status and technology development plans for subsystems below TRL 6 are summarized in Table 14.

Table 14: mDOT technology development needs for components with TRL<6

Component	TRL (mDOT)	Development need
Starshade Deployment Assembly	5	On-ground demonstration of starshade manufacture and deployment with acceptable errors as from tolerance analysis.
Telescope Payload Assembly	5	On-ground validation of telescope payload performance.
ECAPS Thrusters	5	Validation of thruster performance in orbit.
DiGiTaL/GNC	5	Hardware-in-the-loop demonstration of autonomous precise relative navigation and control.
Tx/Rx Module with Patch Antennas	5	On-ground qualification tests.

The individual components are addressed in the following.

Starshade Deployment Assembly. The deployment assembly (hub, motor, linkages, and hinges for petals) is a novel design developed by Tendeg specifically for the mDOT mission. While the materials and components for this design are similar to those used in full-scale starshade designs, an on-ground test campaign is required to verify that the proposed design can be manufactured and deployed with acceptable errors[19].

Telescope Payload Assembly. The telescope payload is a modified version of the Planet Labs PS2 telescope, which now has extensive flight heritage (>100 units on orbit) in the Dove constellation. The modifications include introduction of a Mirrorcle S6180 mirror and secondary detector for image stabilization and a TEC for thermal control. A laboratory prototype of a two-sage attitude control system has been developed and tested at Stanford University[2]. Further on-ground qualification testing is needed as part of mDOT to raise the TRL of the telescope payload to 6.

ECAPS Thrusters. The propulsion system uses HPGP 5N thrusters developed by Bradford ECAPS. The 5N thruster is based on a 1N version with LEO flight heritage from the Skysat 3-7 and PRISMA missions. Development and qualification of the 5N thrusters is coupled with the qualification program for the HPGP 22N thrusters. The first flight-like HPGP 22N thruster was designed and built to substantiate the thruster design, build process, and testing to NASA GSFC PACE mission requirements. This test program was intended to bring the thruster TRL level from 5 to 6. The HPGP 5N and 22N thruster designs will be updated to incorporate the lessons learned during 22N thruster testing (completed in 2017). The HPGP 5N thruster is scheduled to be tested in 2018-2019[20]. Successful completion of this test campaign should bring the 5N thruster TRL level to 6.

Tx/Rx Module with Patch Antennas. The telecommunication system uses a Tx/Rx module and Patch Antennas developed by Cesium, the same manufacturer of the SDR. While the SDR is already at TRL 6, the Tx/Rx module is currently at TRL 5, progressing to TRL 6 upon completion of thermal testing of the existing high-fidelity engineering model. The Patch Antennas are currently at TRL 4, with Cesium in the process of starting manufacturing of the patch antenna's engineering model. The entire telecommunication system (SDR, Tx/Rx Module and Patch Antennas) is planned to complete qualification testing (TRL 8) by end of summer 2019.

DiGiTaL and Formation-Flying Algorithms. The DiGiTaL navigation and formation-flying algorithms are under development at the Stanford's Space Rendezvous Laboratory under two NASA SSTP contracts in collaboration with NASA Ames and GSFC. DiGiTaL uses differential carrier-phase GNSS techniques similar to those deployed on the PRISMA mission which achieved 10cm (3D, rms) relative positioning accuracies at separations from 2m to 50km[16]. However, DiGiTaL aims at centimeter-level relative positioning accuracy (3D, rms) in real-time through improved integer ambiguity resolution algorithms at separations up to 505km. The mDOT mission requires a formation at 500 km separation to autonomously maintain alignment with an inertial target with centimeter-level accuracy and conduct formation reconfigurations to re-align the formation for repeated observations of the same target. To date, these capabilities have only been partially flown and verified in space. The Stanford's Space Rendezvous Laboratory has experience with these algorithms from the flown GRACE, TanDEM-X, PRISMA, BIROS missions. Improved algorithms are currently in development as part of the Autonomous Nanosatellite Swarming using Radio-Frequency and Optical Navigation (ANS) SSTP contract in collaboration with NASA Ames Research Center[21]. It is expected that the TRL of DiGiTaL and formation-flying algorithms will be raised to 7 within two years, through the current Stanford's research and development program and scheduled flight demonstrations on the Starling1 mission, which is scheduled for launch in 2020[22].

CONCLUSION

This paper presented a pre-phase A system design of the miniaturized Distributed Occulter Telescope (mDOT) conducted by Stanford University and NASA Ames research centers under contract from the NASA Mission

Directorate. mDOT will provide unprecedented detection and direct measurements of brightness of extrasolar dust disks at short visible to ultraviolet wavelengths. The baseline mission will observe over 15 targets using a starshade for high-contrast imaging, blocking the target star with a specially shaped free-flying occulter to allow nearby objects to be detected. mDOT operates on a much smaller scale than flagship NASA missions, with an autonomous formation of two small satellites in sun-synchronous low Earth orbit. An occulter-smallsat (246kg, 192W) carries a precisely manufactured 3m-diameter starshade and a telescope-cubesat (6U, 12kg, 40W) carries a 10cm-diameter telescope. The satellites are launched combined as a secondary payload for a total mission lifetime of 1.1 years. After launch, the occulter-smallsat ejects the telescope-cubesat and maneuvers to establish the desired relative orbit, leaving the spacecraft at slightly different longitudes of ascending node. Relative eccentricity and inclination vector separation provides the baseline for scientific observations at the equator (500 km) and a minimum safe distance perpendicular to the flight direction at all times (>1km). The starshade suppresses the light of the target star by 10^{-7} or more. During a science pass, high-ISP green propellant thrusters on the occulter-smallsat maintain the formation, while differential GNSS is used for cm-accurate relative navigation. Earth's oblateness perturbations are used to precess the orbits and acquire the science targets over the mission lifetime at minimal propellant cost. The presented point design closes with healthy technical margins on all resources and proves the feasibility of a small starshade mission in Earth orbit. At the same time, the study identifies technical risks and technology gaps that need to be addressed to pave the way for an actual mission. More importantly, the starshade deployment assembly, the telescope payload assembly, and the guidance, navigation, and control software need to be matured to TRL 6. The mDOT mission addresses key NASA science objectives and provide the unique opportunity to mature starshade techniques for future exoplanet missions.

ACKNOWLEDGMENTS

Many thanks to the following members of the ARC Mission Design Centre:

- Brittany Wickizer – System Engineer
- Daniel Larrabee (former member) – System Engineer
- Peter Paragas – System Engineer
- Sonny Hwang – GNC Engineer
- Timothy Snyder – Mechanical engineer

This work was sponsored by NASA Grant 80NSSC19K0142.

REFERENCES

1. Boshuizen, C., Mason, J., Klupar, P., and Spanhake, S., "Results from the Planet Labs Flock Constellation," Proceedings of the 28th AIAA/USU Conference on Small Satellites, Logan, UT, August 2014.
2. Beierle, C., Norton, A., Macintosh, B., and D'Amico, S., "Two-Stage Attitude Control for Direct Imaging of Exoplanets with a CubeSat Telescope," Proceedings of the SPIE Astronomical Telescopes + Instrumentation Conference, Austin, TX, June 2018.
3. Glassman, T., Lo, A. S., Arenberg, J., Cash, W., and Noecker, C., "Starshade Scaling Relations," Proceedings of the SPIE Optical Engineering + Applications Conference, San Diego, CA, August 2009.
4. Koenig, A. W., Macintosh, B., and D'Amico, S., "Formation Design of Distributed Telescopes in Earth Orbit for Astrophysics Applications," Journal of Spacecraft and Rockets, 2019. In press.
5. Koenig, A. W., D'Amico, S., Macintosh, B., and Titus, C. J., "A Pareto-Optimal Characterization of Miniaturized Distributed Occulter/Telescope Systems," Proceeding of the SPIE Optics + Photonics Conference, San Diego, CA, August 2015.
6. Shaklan, S. B., Noecker, M. C., Glassman, T., Lo, A. S., Dumont, P. J., Kasdin, N. J., Cady, E. J., Vanderbei, R., and Lawson, P. R., "Error Budgeting and Tolerancing of Starshades for Exoplanet Detection," Proceedings of the SPIE Astronomical Telescopes + Instrumentation Conference, San Diego, CA, June 2010.
7. Shaklan, S. B., Marchen, L., Cady, E., Ames, W., Lisman, P. D., Martin, S. R., Thomson, M., and Regehr, M., "Error budgets for the Exoplanet Starshade (Exo-S) Probe-Class Mission study," Proceedings of the SPIE Optical Engineering + Applications Conference, San Diego, CA, August 2015.
8. Giralo, V. and D'Amico, S., "Distributed Multi-GNSS Timing and Localization for Nanosatellites," Proceedings of the ION GNSS+ Conference, Miami, FL, September 2018.
9. Koenig, A. W., D'Amico, S., Macintosh, B., and Titus, C. J., "Optimal Formation Design of a Miniaturized Distributed Occulter/Telescope in Earth Orbit," Proceedings of the AAS/AIAA

Astrodynamics Specialist Conference, Vail, CO, August 2015.

10. D'Amico, S. and Montenbruck, O., "Proximity Operations of Formation Flying Spacecraft using an Eccentricity/Inclination Vector Separation," AIAA Journal of Guidance, Control, and Dynamics, Vol. 29, No. 3, pp. 554-563, 2006.
11. Anflo, K. and Möllerberg, R., "Flight demonstration of new thruster and green propellant technology on the PRISMA satellite," Acta Astronautica, Vol. 65, No. 9-10, pp. 1238-1249, 2009.
12. Mulkey, H. W., Maynard, A. P., and Anflo, K., "Green Propulsion Advancement and Infusion," Proceedings of the 3AF Space Propulsion Conference, Seville, Spain, May 2018.
13. "ESPA User's Guide," Moog, Inc., Space and Defense Group, November 2018. URL: https://www.moog.com/content/dam/moog/literature/Space_Defense/spaceliterature/structures/Moog_ESPA_UsersGuide.pdf
14. Macintosh, B. et al., "mDOT Concept Study Report," Stanford University, June 2019.
15. Sorgenfrei, M. and Lewis, B. S., "BioSentinel: Enabling CubeSat-Scale Biological Research Beyond Low Earth Orbit," Proceedings of the Interplanetary Small Satellite Conference, Pasadena, CA, April 2014.
16. D'Amico, S., Ardaens, J.-S., and DeFlorio, S., "Autonomous Formation Flying based on GPS – PRISMA flight results," Acta Astronautica, Vol. 82, No. 1, pp. 69-79, 2012.
17. Koenig, A. W. and D'Amico, S., "Real-Time Algorithm for Globally Optimal Impulsive Control of Linear Time-Variant Systems," IEEE Transactions on Automatic Control, 2019. Submitted.
18. Koenig, A. W., "Formation Design of Distributed Telescopes in Earth Orbit with Application to High Contrast Imaging," Stanford University, PhD Thesis, 2019.
19. Arya, M. et al., "Starshade mechanical design for the Habitable Exoplanet Imaging Mission Concept (HabEx)," Proceedings of the SPIE Optical Engineering + Applications Conference, San Diego, CA, August 2017.
20. Dinardi, A., Anflo, K., and Friedhoff, P., "On-Orbit Commissioning of High Performance Green Propulsion (HPGP) in the SkySat Constellation," Proceedings of the 31st AIAA/USU Conference on Small Satellites, Logan, UT, August 2017.
21. Stacey, N. and D'Amico, S., "Autonomous Swarming for Simultaneous Navigation and Asteroid Characterization," Proceedings of the AAS/AIAA Astrodynamics Specialist Conference, Snowbird, UT, August 2018.
22. Sanchez, H., Mcintosh, D., Cannon, H., Pires, C., Sullivan, J., D'Amico, S., and O'Connor, B., "Starling1: Swarm Technology Demonstration," Proceedings of the 32nd AIAA/USU Conference on Small Satellites, Logan, UT, August 2018.